

Fabrication and *Ex-vivo* Evaluation of Olanzapine Nanoparticles Based Dissolved Microneedle for Transdermal Delivery

Abulfadhel J. Neamah Al-Shaibani¹  and Mowafaq M. Ghareeb^{*2} 

¹Department of Pharmaceutics, College of Pharmacy, University of Kufa, Najaf, Iraq.

²Department of Pharmaceutics, College of Pharmacy, University of Baghdad, Baghdad, Iraq.

*Corresponding author

Received 29/10/2023, Accepted 28/2/2024, Published 25/10/2025



This work is licensed under a Creative Commons Attribution 4.0 International License.

Abstract

Olanzapine (OLZ), a second-generation antipsychotic medication used to treat schizophrenia, its 60% oral bioavailable, which is inadequate because of first-pass hepatic metabolism. Therefore, the purpose of current study is to fabricate and evaluate olanzapine nanoparticles loaded dissolving microneedles for drug delivery through the skin to circumvent the challenges associated with oral drug administration and to make medicine administration easier for individuals with schizophrenia. Nanoprecipitation method was applied to prepare nanoparticles by using different polymers with various ratios. Nanoparticles were assessed by several investigational studies such as particle size, polydispersity index (PDI), entrapment efficiency, zeta potential and an *in vitro* release study. Field emission scanning electron microscope (FESEM) was used to screen nanoparticles morphology. Dissolved Microneedles (MNs) patch was fabricated by placing OLZ nanodispersion in cavities of polydimethylsiloxane (PDMS) micromolds, followed by molding the polyvinyl alcohol (PVA) and polyvinylpyrrolidone (PVP-K30) as polymeric solution to form the matrix of MNs, the prepared MNs patches were evaluated for morphology, mechanical strength, drug content and permeation study. The results revealed that OLZ nanoparticles was in nano-size scale ranged from 70.12 nm to 344 nm, PDI values range (0.152-0.404), entrapment efficiency ranged from 53.2% to 78.4%, the highest zeta potential value was (-19.01 mV) for OLZ nanoparticle (OLZ-5), that exhibits a greater and significant drug release ($P < 0.05$). FESEM shows spherical shape of nanoparticle with size similar to that obtained by zetasizer. According to the results of nanoparticles, the formula (OLZ-5) considered as optimized formula and utilized for fabrication of MNs. The results of MN fabrication indicate that MN-4 exhibits a sharp needle with good mechanical strength according to texture analysis, drug content (98.52%), according to the results of the permeation testing, MN-4 penetrates the skin 5.16 times more efficiently than a simple patch. In conclusion the MNs patch (MN-4) represent the promising formula to avoid the obstacles that concerned with oral dosage form of drug and may improve patient compliance and drug bioavailability.

Keywords: Olanzapine, Nanoparticles, Solubility, Polymers, Microneedle.

Introduction

Nanoparticles considered as solid particles that range in size from 10 to 500 nm, in which the drug may dissolve, be trapped, or be encapsulated within nanoparticle matrix ⁽¹⁾. Nanoparticle loaded drug represent an advance system for delivery of several drugs for treatment of different diseases due to its advantages such as better improvement in dissolution rate of drugs, control drug release, higher loading of drug, delivery of drugs to the target site and protection of drugs against enzymatic degradation ⁽²⁾. Despite the administration of drug loaded nanoparticle using different routes including intravenous, ophthalmic, and oral, the transdermal delivery of nanoparticles attracted a lot of interest because of ability to improve patient compliance by decreasing the pain that linked with usage of hypodermic needle, prevention of first-pass hepatic metabolism, self-administration and protection

against enzymatic degradation of drugs ⁽³⁾. Stratum corneum serves as a functional barrier for drug penetration and delays drug penetration, slows the therapeutic action of medications, making it the primary obstacle to drug delivery via the skin. Various techniques have been utilized to enhance the drug's penetration into the layers of the skin, including iontophoresis, ultrasound, and microneedles (MNs) ⁽⁴⁾. MNs considered as innovative physical technique, which developed to overcome the barrier of skin that represented by stratum corneum and enhance the drug penetration via skin into systemic circulation. MNs defined as micro-sized needle arranged in arrays capable of producing pores in skin and enhance the delivery of nanoparticles through these created pores, so, several advantages associated with MNs such as better patient compliance, high permeation of drug,

self-administration and improved bioavailability of drugs ^(5,6). Therefore, compared to nanoparticles alone, nanoparticle loaded MNs enable transdermal transport of nanoparticles; this is a function of the micropores that MNs form ⁽⁷⁾. There are several kinds of MNs used for drug delivery, including solid, coated, dissolved, and hydrogel MNs. These MNs vary in their manufacturing processes, drug delivery tactics, and materials used. ^(8,9) Dissolving MNs received great attention because of its advantages such as high drug loading, easy fabricated by micro molding and doesn't produce biohazard waste, it can be fabricated by using biocompatible and biodegradable polymer for encapsulating the drug, interstitial fluid dissolves the tips of MNs, releasing the content of dissolved MNs instantly after the medicine is inserted into the skin. ^(10,11) OLZ is a second-generation antipsychotic medication with molecular weight (312.44 g/mol) and molecular formula (C₁₇H₂₀N₄S) as in Figure 1. Because of its limited solubility and substantial first-pass hepatic metabolism, OLZ has a 60% oral bioavailability. ⁽¹²⁾ So, the purpose of current study is to formulate OLZ as nanoparticle dissolved microneedle for transdermal delivery and this could improve patient compliance and increase the drug's bioavailability.

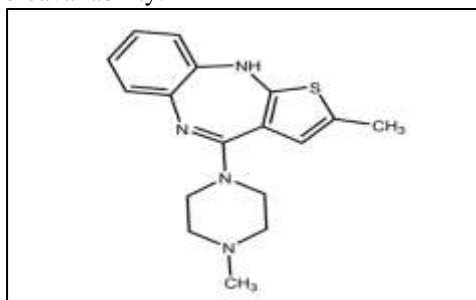


Figure 1. OLZ chemical structure ⁽¹³⁾.

Materials and Methods

Materials

OLZ for laboratory use was acquired from Hyperchem, China; polymers such as polyvinylpyrrolidone (PVP) with varying molecular weights, such as PVP-K30 and PVP-K15, were acquired from Provizer Pharma, India; polyvinyl alcohol (PVA) were procured from Rhom Pharma, Germany; Soluplus® polymer was acquired from BASF, Germany; Sigma-Aldrich, Germany, provided the methanol solvent; and all other analytical-grade solvents and chemicals were used.

Methods

Preparation of OLZ nanoparticles

The bottom-up, or nanoprecipitation approach was used to create OLZ nanoparticles. Using this method, OLZ (10 mg) is dissolved in 3 ml of organic solvent (absolute methanol). A syringe pump is then used to drop the organic phase into aqueous phase (deionized water with stabilizer) at a rate of 1 ml per minute. while being continuously stirred at 600 rpm. The precipitation of nanoparticles occurs immediately after dropping. To allow the organic solvent to evaporate, the resultant nanosuspension is placed on a magnetic stirrer for an hour ⁽¹⁴⁾. The composition of nanoparticles was presented in Table 1.

Table 1. The OLZ nanoparticle's variables and composition.

Code of formula	OLZ* (mg)	Polymer (Stabilizer)	Amount of Stabilizer(mg)	D:P* ratio	O:A* ratio
OLZ-1	10	PVP-K15	10	1:1	3:30
OLZ-2	10	PVP-K15	20	1:2	3:30
OLZ-3	10	PVP-K15	30	1:3	3:30
OLZ-4	10	Soluplus®	10	1:1	3:30
OLZ-5	10	Soluplus®	20	1:2	3:30
OLZ-6	10	Soluplus®	30	1:3	3:30
OLZ-7	10	PVA	10	1:1	3:30
OLZ-8	10	PVA	20	1:2	3:30
OLZ-9	10	PVA	30	1:3	3:30

*Where olanzapine, Drug; Polymer and Organic: Aqueous ratio as OLZ, D: P, and O: A respectively.

Nanoparticles Characterization

Polydispersity index (PDI) and particle size determination

The PDI and particle size of nanoparticles were measured using the Zeta sizer (Malvern Instruments Ltd., United Kingdom). The instrument measured the amount of light scattered by the sample's particles at room temperature at a scattering angle of 90°C. After analysis, it was discovered that the PDI was responsible for the homogeneity and particle size distribution within prepared formula⁽¹⁵⁾.

Zeta potential Screening

The zeta potential of prepared OLZ formulations was screened by zeta sizer (Malvern Instruments Ltd, United Kingdom)⁽¹⁶⁾. A triplicate measurement was done.

Entrapment Efficiency (EE%)

Centrifugation 5 ml of drug nanosuspension at 3000 rpm for 20 minutes in tube with Ultra centrifugation and molecular cut off (MWCO) 10 kDa, the EE% of OLZ nanodispersion was estimated indirectly, which involves determining the free OLZ in the dispersion medium⁽¹⁷⁾. By UV-visible spectrophotometer set at 270 nm and the following formula, the untrapped concentration of OLZ found in ultrafiltration was diluted⁽¹⁸⁾.

$$EE\% = \frac{WT-WF}{WT} \times 100$$

Equation 1

Where, WF is the weight of free OLZ that was measured in the supernatant layer following ultrafiltration, and WT is the (total) initial weight of medication utilized. Three separate measurements were made, and the results were reported as mean \pm SD.

In vitro release study

OLZ powder and its nanodispersion were released *in vitro* by introducing 3 mg of pure medication and adequate OLZ nanodispersion containing 3 mg of drug to a dialysis bag 8000–14000 Da⁽¹⁹⁾. A dissolution equipment USP-II (paddle) was used to release the medication with temperature 37°C \pm 0.5 and revolving at 50 rpm. A specified sample volume (5 ml) was taken at intervals of 5, 10, 15, 20, 30, 40, 50, 60, 70, 80, and 90 minutes after the sealed dialysis bag was immersed in 500 ml of dissolution medium, which

is phosphate buffer pH7.4 that included 0.2% tween 20. To keep the sink condition stable, buffer was added to each withdrawn volume. Filter membrane (0.45 μ m) was used for filtering the samples and drug quantity was measured by using UV-visible spectrophotometer at 252 nm⁽²⁰⁾. Triplicate measurement was done.

surface morphology of nanoparticle

OLZ nanoparticles were examined for morphology using a field emission scanning electron microscope (FESEM) (HITACHI S-4160, Japan).

Powder X-ray diffraction study

A mixture of OLZ and polymer, pure OLZ, and OLZ nanoparticles were subjected to powder X-ray diffraction examination to ascertain the crystallinity nature of these samples. The X-ray diffractometer (XRD-6000, Shimadzu, Japan) was used for the analysis; its operating voltage and current were 40 (kV) and 30 (mA), respectively. Samples were scanned at 2 Theta from 0-80° at a rate of 5°/min⁽²¹⁾.

Differential scanning calorimetry

DSC is a thermal analysis method, through which, 5 mg of pure OLZ powder and a chosen lyophilized formula were placed in the pan of DSC-60 Shimadzu, Japan, that made of aluminum, and heated at 10°C/min between 50 and 250 °C with a nitrogen flow of 40 ml/min.^(22,23)

MNs Fabrication

There are 225 conical needles in the mold of the dissolved MNs patch. They are arranged in a 15 \times 15 cm array with dimensions of 500 μ m for height, 200 μ m for base diameter, and 1500 μ m for needle pitch. It is around 4 cm². The mold of MNs was obtained from Micropoint company in Singapore.

Preparation of matrix for MNs

The dissolved MN matrix was made up of two polymers (PVA and PVP-K30). Two grams of one polymer or mixture of two polymers in various ratios were collected, dissolved in 20 milliliters of distilled water, plasticized with 5% (w/w) glycerin, and heated for two hours at 50 °C to produce the polymeric solution. The resulting polymeric solution was placed in a sealed glass container and allowed overnight to obtain a clear, bubble-free solution suitable for MN manufacturing⁽²⁴⁾. Table 2 describes the composition of MNs.

Table 2. Formula composition for MNs.

Code of Formula	PVA (gm)	PVP-K30 (gm)	Glycerin % (w/w)	DW (ml)	Polymeric Solution (%)
MN-1	2		5	20	10
MN-2		2	5	20	10
MN-3	1	1	5	20	10
MN-4	1.25	0.75	5	20	10
MN-5	1.5	0.5	5	20	10
MN-6	1.75	0.25	5	20	10

Drug loading in MNs mold

There are two steps involved in loading drug into the mold of MNs. The first is loading OLZ nanodispersion (3 ml of nanodispersion contain 1 mg of drug) into the mold cavities using a sonicator (Hwashin Tech., Korea) for one hour. The mold is then placed in a degassed desiccator for twenty-four hours to dry. After that, the polymeric solution is sonicated for half an hour after being cast in the mold. The mold is then allowed to dry for twenty-four hours in a degassed desiccator. This guarantees that the MNs' tip has the highest concentration of medication.⁽²⁵⁾

MNs Patch Characterization

MNs morphology

Along with examining the MNs' morphology under a digital microscope (Depstech, China), Image J software was utilized to compare the MNs' length, height, width, and interspacing to the master mold.

Drug Content

The amount of OLZ in MNs was measured by placing the microneedle patch for each formulation in mixture solvent (25 ml of DW and 25 ml of methanol) on a magnetic stirrer for three hours. After the solution has been filtered and diluted with the proper solvent, drug quantity was assessed by utilizing UV-visible spectrophotometer set at 270 nm.⁽²⁶⁾

Mechanical strength of MNs

A test of distance force station (Testometric, TA.XT. PLUS, UK) was used to apply a high force parallel to the MNs' axis in order to determine their mechanical strength. By monitoring the force and distance while the MNs arrays were pushed on a metal surface using a test station at a speed of 0.5 mm/sec and a target force of 3059.1 gm (32 N), which corresponds to finger human force and a distance of 5 mm, a stress vs strain curve was created. When the force abruptly dropped after needle failure, the maximum force delivered just prior to the drop was regarded as the needle failure force.⁽²⁷⁾

Permeation Study

An ex vivo permeation investigation was conducted on rabbit abdominal skin bought from the University of Baghdad's College of Pharmacy's animal house. The study used OLZ nanoparticles that dissolve MNs and a basic conventional patch. In a Franz cell, the skin is sandwiched between the donor and receptor compartments, with the stratum corneum facing upward. 3.14 cm² of skin surface area was available for the medication to distribute effectively. The receptor compartment keeps the sink situation stable. Using light pressure, the MNs and regular patch containing 1 mg of OLZ were applied to the skin. At intervals of 15, 30, 45, 60, 90, 120, 150, 180, 210, 240, 270, and 300 minutes, a 2-

milliliter aliquot sample was removed from the receptor chamber and replaced with new medium to maintain sink condition. Samples were analyzed at 252 nm using a UV-visible spectrophotometer. The apparent permeation is obtained by constructing the total drug amount permeated against time interval^(28,29).

Statistical analysis

Excel 2016 was used to analyze data from at least three separate tests. The standard deviation is included with all means. When necessary, one-way analysis of variance (ANOVA) was carried out. At $P < 0.05$, statistical significance was taken into account.

Results and Discussion

Analysis of particle size and polydispersity index (PDI)

According to Table 3 data, the nanoparticle size ranged between 70.12 and 344 nm, while the PDI ranged between 0.152 and 0.404. The distribution and homogeneity of drug nanoparticles within a sample are considered to be crucially investigated by PDI. OLZ nanoparticles are therefore considered to have mid-range polydispersity based on PDI data because their PDI values are less than 0.7^(30,31).

Zeta potential Screening

One physical characteristic of nanodispersion is the zeta potential, which is the potential difference between the bulk solution (dispersing medium) and the surface of the hydrodynamic shear (slipping plane)⁽³²⁾. As explained in Table 3, the results show reduced zeta potential values for all OLZ nanoparticle formulations; the values fell between -5.59 and -16.02 mV. The zeta potential was used to express the repulsion between adjacent and particles with similar charge in a dispersing system. When stabilization is based on steric stabilizers, the observed zeta potential is less because the stabilizer's adsorption layer shifts the plane of shear, where the zeta potential is measured, far from the particle surface. Consequently, OLZ-5 zeta potential was adequate for stability.

Entrapment efficiency (EE%)

The relationship between the ratio of polymer and EE% is indicated by the entrapment efficiency of nanoparticles; that is, when the ratio of polymer rose, Significantly, the entrapment efficiency rose ($P < 0.05$). The reason for this procedure is because a higher stabilizer ratio enhances polymer attachment to the nanoparticle shell, increasing the stabilizer solution's viscosity and delaying drug diffusion into the external phase, resulting in high entrapment efficiency.^(35,36) Table 3 demonstrates the raising of EE%, as stabilizer ratio increased from (1:1) to (1:2) and (1:3).

Table 3. Zeta potential, PDI, entrapment efficiency, and particle size of prepared nanoparticles.

Formula Code	Average particle size (nm)	PDI	Zeta potential (mV)	EE%*
OLZ-1	70.12±9.31	0.30±0.090	-6.04±0.12	53.2±3.78
OLZ-2	98.32±4.66	0.282±0.180	-12.4±0.15	72.6±6.11
OLZ-3	111.86±9.12	0.205±0.040	-5.59±0.09	74.5±3.81
OLZ-4	77.98±2.84	0.152±0.110	-12.09±2.1	68.2±4.87
OLZ-5	122.1±5.45	0.240±0.070	-15.52±1.8	78.4±5.46
OLZ-6	344±24.85	0.404±0.068	-15.85±0.11	81.1±6.13
OLZ-7	111.73±16.0	0.242±0.065	-10.65±0.23	65.3±2.67
OLZ-8	171.8±35.5	0.385±0.325	-16.2±0.78	72.6±6.93
OLZ-9	164.3±23.3	0.231±0.210	-11.3±0.11	70.1±4.24

Results as expressed as (mean ± SD, n=3).

In vitro release study

The chosen formulations OLZ-8, OLZ-5, and OLZ-2 with various polymer types were put through the study of release screening process based on nanoparticles characterization studies, which include particle size, zeta potential, and entrapment efficiency⁽³⁷⁾. The obtained results indicate that all preparations show higher release and significant ($P<0.05$) when compared to the pure medicine. The dissolving rate of particles is regarded as surface area function of particles, which is explained by the Noyes-Whitney equation, which indicates that as a particle's size reduces, its solubility increases, elevating the rate of dissolution. This description is in line with the results of Ahmed H. Ali et al. (2019), who created a nanosuspension of atorvastatin

calcium utilizing a variety of polymers and the nanoprecipitation method⁽³⁸⁾. The kind of polymer also influences drug release from nanoparticles, which is influenced by the mechanical characteristics of the polymer and the drug-polymer interaction. Consequently, Soluplus® is an amphipathic co-polymer that reduces interfacial tension by acting as a wetting agent and surfactant. Therefore, when compared to other PVP-K15 and PVA formulations, OLZ-5 shows a greater and significant release ($P<0.05$)⁽³⁹⁾. This is explained by the fact that, in contrast to other polymers, soluplus® enables water-surface interaction that maintains the smallest nanoparticle size by enabling quick OLZ dissolution and release. Figure 2 detailed the OLZ nanosuspensions' *in vitro* release profile.

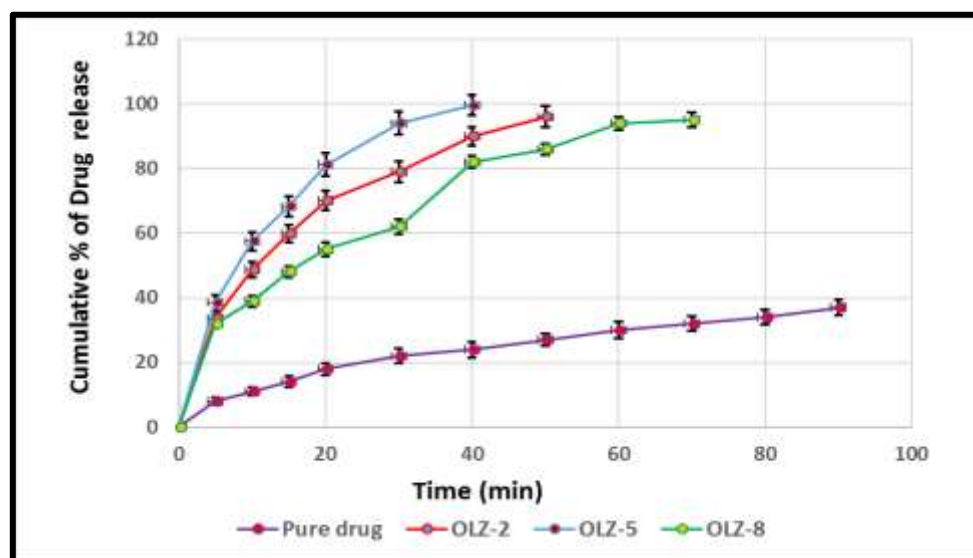


Figure 2. *In vitro* release profile of OLZ nanoparticles.

Optimized formula of OLZ nanoparticles

The results of characterization studies on all formulations of olanzapine nanoparticles, including zeta potential, entrapment efficiency, PDI, and particle size, indicate that OLZ-5 is an optimized formula because it has a significant drug release ($P < 0.05$), a higher entrapment efficiency (78.4) than

other formulations, a lower particle size (122.1 nm) as shown in Figure 3, zeta potential value (-15.52 mV) as shown in Figure 4, a higher value of PDI (0.24) that shows a uniform distribution of particle size within preparation.

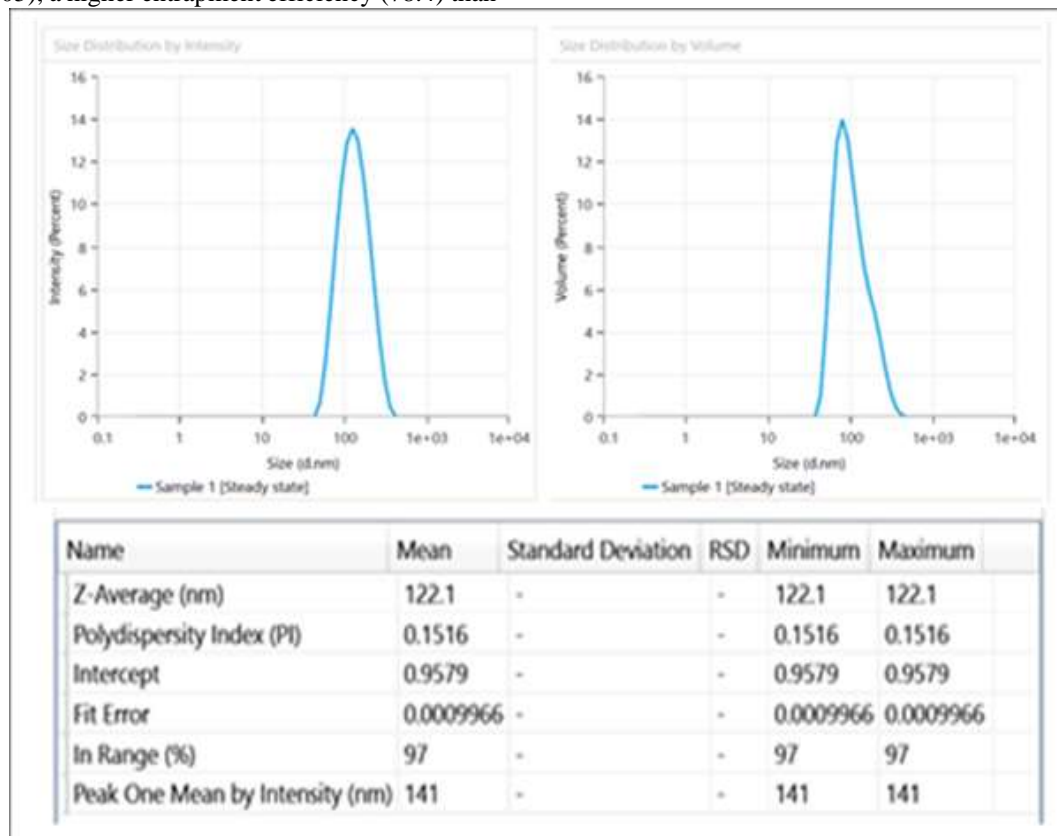


Figure 3. Particle size of OLZ nanoparticles (OLZ-5).

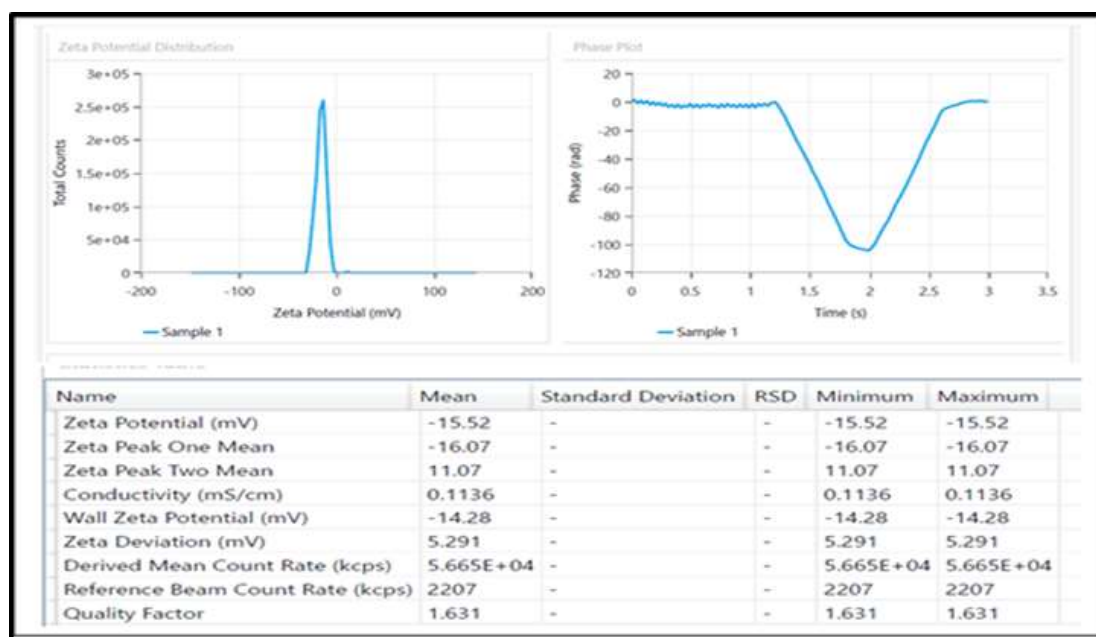


Figure 4. Zeta potential of nanoparticles (OLZ-5).

Surface morphology of OLZ nanoparticle

According to field emission scanning electron microscopy (FESEM). Figure 5 reveals that

the nanoparticles was spherical in shape and roughly the same size as that determined by a zeta sizer.

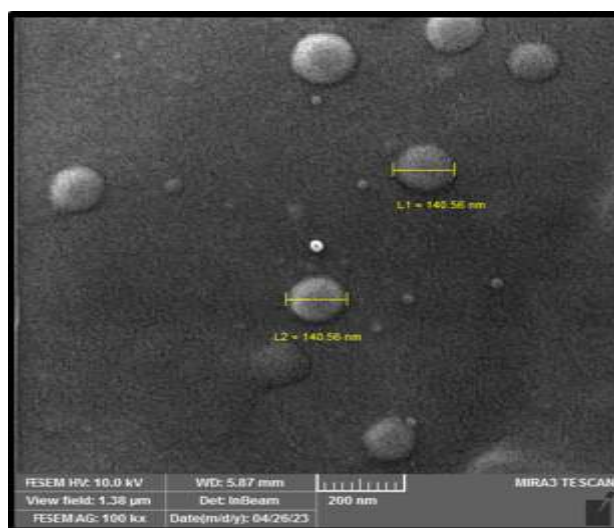


Figure 5. FESEM of nanoparticle (OLZ-5).

Powder X-ray diffraction screening

Pure OLZ X-ray diffractogram exhibited a sharp peak with high intensity at angle 2 Theta of 9°, 20°, 21°, 22° and 24°, which indicate the crystalline nature of drug. The physical mixture of drug and polymer in ratio (1:2) exhibited the same diffractogram but with the same sharp peaks but in reduced intensity and this indicates the remaining of

drug in crystalline nature and there wasn't interaction between the polymer and drug. In OLZ nanoparticle (OLZ-NP) exhibit disappearance of some sharp peaks specially 2 Theta of 9°, 21° and 22° in addition to reduce intensity of other peaks, this indicates a reduction in crystallinity of OLZ^(40,41). Figure 6 explains the X-ray diffractogram of pure drug, physical mixture and OLZ-NP.

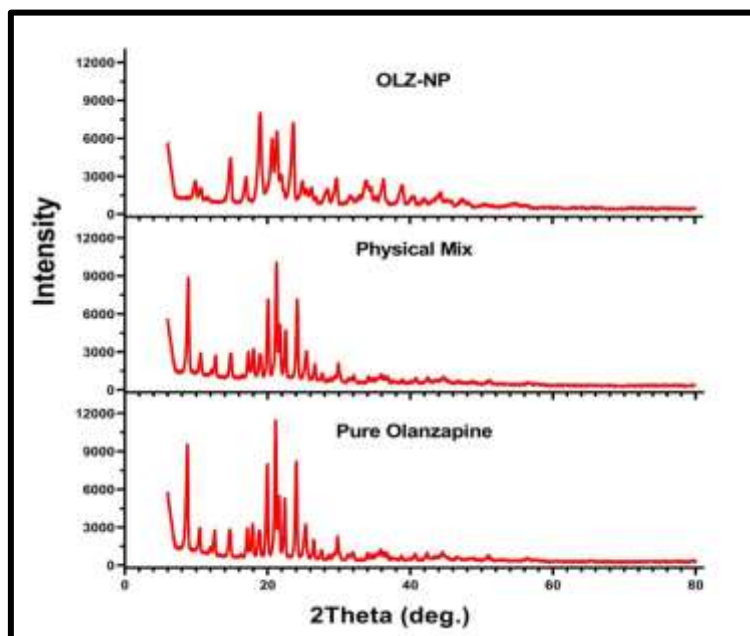


Figure 6. X-ray diffraction of physical mixture (drug: soluplus®), pure OLZ, and (OLZ-NP).

Differential scanning calorimetry

For pure powder of OLZ, there is a noticeable endothermic peak in DSC screening at 198.38 °C, which represents the melting point of OLZ and is the same as the reference readings (196 °C to 198 °C) ^(42,43). Because olanzapine's crystallinity is reduced,

the DSC measurements of the lyophilized nanoparticle OLZ-5 show a broad endothermic peak with shifting ⁽⁴⁴⁾. Figures 7 and 8, respectively, provided an explanation of the DSC thermogram of pure OLZ and OLZ nanoparticle OLZ-5.

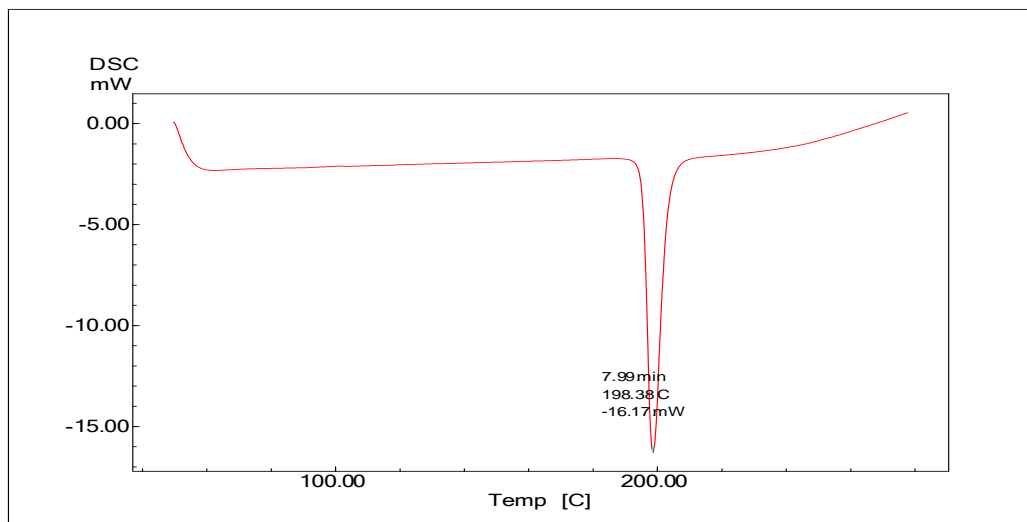


Figure7. DSC thermogram of OLZ pure powder.

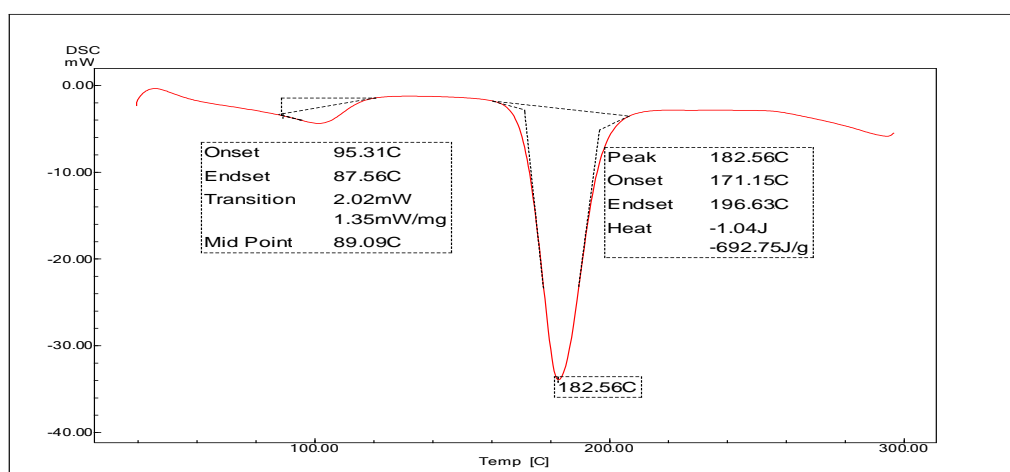


Figure 8. DSC thermogram of optimized OLZ nanoparticle (OLZ-5).







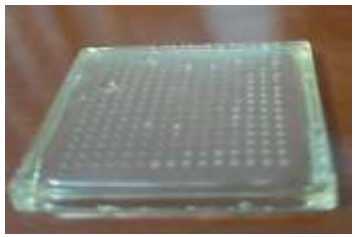


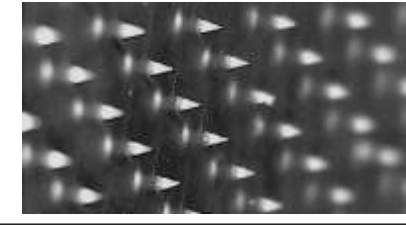


MNs characterizations

Morphology of MNs

The findings demonstrated that, depending on the makeup of the polymeric solutions that comprise the matrix of MNs patches, different formulations of manufactured MNs produce different shapes when compared to the master mold. To verify the patch tips, a hand digital microscope can screen the shape of artificially dissolved MNs with varying compositions ⁽⁴⁵⁾. The morphology of prepared MNs with varying contents was described

in Table 4. Both MN-2 and MN-1, which were composed of PVP-K30 and PVA, respectively, displayed a bubbles in the patches and a short needle. This could be because MN-1 high viscosity of polymer delayed the formation of a needle that resembled the master mold, in contrast, patches composed of a blend of polymers in different proportions included sharp needles that mirrored the original mold and had perfect plasticity because of the existence of plasticizer (glycerin), which had a chance for penetration of skin layers ⁽⁴⁶⁾.

Table 4. The shape of MNs patches with different composition.

Formula Code	MNs Patch	MNs with digital microscope
MN-1		
MN-2		
MN-3		
MN-4		
MN-5		
MN-6		

Drug content

The content of OLZ in all MNs patches were found in range (94.39 ± 2.40 to 98.52 ± 3.71), this results revealed that a little of drug lost during formulation. Table 5 exhibits the results of drug content of all MNs patches.

Table 5. Drug content of MNs patches, where

Formula code	Drug content%
MN-1	95.31 ± 4.20
MN-2	94.39 ± 3.11
MN-3	97.56 ± 2.13
MN-4	98.52 ± 3.71
MN-5	98.12 ± 1.42
MN-6	96.76 ± 4.12

results as (mean \pm SD, n=3)

Mechanical strength of MNs

A moderate effect has been observed when drug nanoparticles are added to a solution of polymers during the production of MNs arrays. The ability of MNs patches to penetrate the skin's stratum corneum, which is dependent on the needles' mechanical strength, is what gives them their therapeutic effect⁽⁴⁷⁾. The mechanical strength screening findings showed no symptoms of breakage in any of the MNs patches. The strongest materials are MN-5, MN-4, and MN-3 in terms of their relative forces. According to the mechanical strength test, as the quantity of PVPK-30 grew, elasticity increased and the force required for the fracturing needle reduced⁽⁴⁸⁾. The MNs patch needle got harder and more rigid after the PVA polymer was injected, and it took more force to break.⁽⁴⁹⁾ The test of texture for the MNs patch with the highest force (MN-4) is shown in Figure 9, which plots force (N) against distance (mm). Analyzer of texture (TA-XT2, UK) generated this diagram in compression mode using the previously described steps.⁽⁵⁰⁾

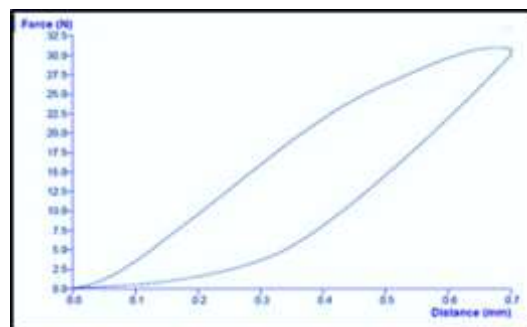


Figure 9. Report of texture analysis of (MN-4).

Ex-vivo study screening

According to the results of the *ex vivo* study, after three hours, OLZ penetration from MN-5 and MN-4 was 58.2%, and 76.4%, respectively. This could be related to the amount of PVP-K30, which means that the more PVP there is in the patch, the more soluble the needle will be in the skin. This is because PVP is hygroscopic, unlike PVA, which causes the needle to be rigid within the patch.⁽⁵¹⁾ The permeation of drug from simple ordinary patch was 22.7%, so, in comparison to the basic patch, the MN patch exhibits increased and substantial ($P < 0.05$) penetration. Construction the drug cumulative amount penetrated per surface area against time interval yielded the steady state flux (Jss), which is represented by straight line slop. Consequently, the MNs patch flux was $53.28 \pm 3.21 \mu\text{g}/\text{cm}^2\cdot\text{h}$ for MN-4 and $46.5 \pm 4.52 \mu\text{g}/\text{cm}^2\cdot\text{h}$ for MN-5, whereas the flux of routine simple patch was $10.32 \pm 1.31 \mu\text{g}/\text{cm}^2\cdot\text{h}$. This shows that, in comparison to a simple patch, MN's patches MN-4 and MN-5 have enhanced their penetration by 5.16 and 4.5 times, respectively. Figure 10 describes the permeation profile from MNs and simple patches. Permeability coefficient (Papp) and steady state flow (Jss) and were shown in Table 6.

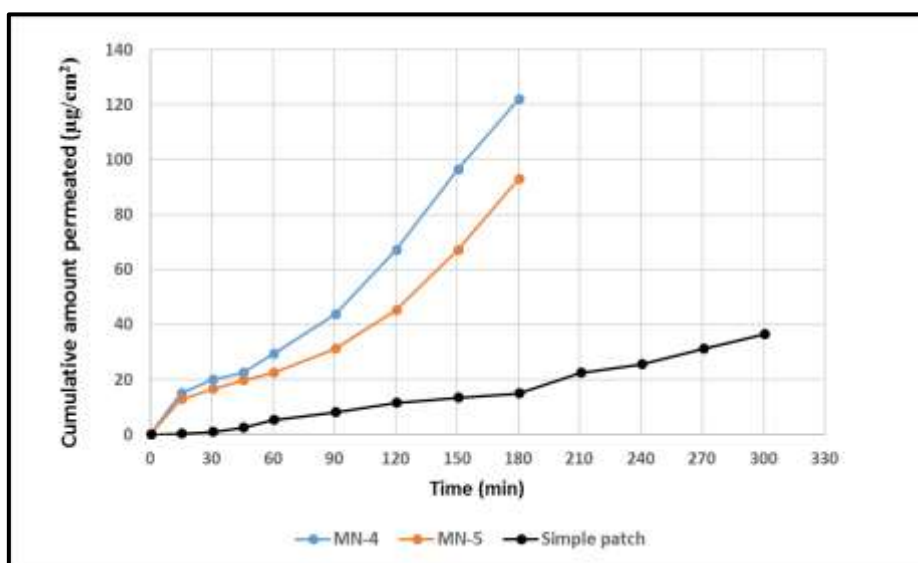


Figure 10. Profile of MNs and simple ordinary patch permeation.

Table 6. Parameters of permeation of OLZ dissolved microneedle, the results as (mean± SD, n=3).

Formula Code	Flux (J_{ss}) ($\mu\text{g}/\text{cm}^2\cdot\text{h}$)	Permeability coefficient (P) (cm/hr)
MN-4	53.28±3.21	0.1065±0.210
MN-5	46.5±4.52	0.093±0.010
Simple patch	10.32±2.13	0.0206±0.007

Conclusion

OLZ nanoparticles were made by the nanoprecipitation method and then put to a polymeric solution to produce a dissolved MNs patch for transdermal distribution. With 10 mg of the drug and 20 mg of soluplus® as a stabilizer, the optimized nanoparticle formula OLZ-5 shows better drug release (99.8%) than pure drug (38.2%), as well as average size of particles (122 nm±5.45), PDI (0.24), and EE% (78.4±5.46). As a result, a polymeric mixture of PVP and PVA in various proportions is employed. One prospective solution to the problems with taking drugs orally is the dissolved microneedle (MN-4). As a result, the MN-4 may increase the drug's bioavailability and enhance patient compliance. In contrast to basic patches, the study of *ex vivo* s demonstrates that MNs (MN-4) have greater penetration and higher flux by 5.16 times.

Acknowledgment

We are grateful to the University of Baghdad's College of Pharmacy's pharmaceuticals department for helping us finish this study.

Conflicts of Interest

This study did not involve any conflicts of interest.

Funding

The authors don't receive financial support from any institution.

Ethics Statements

This research has an ethical approval from an ethics committee in College of Pharmacy, University of Baghdad. The approval number (REAFUBCP932023A) in 29-3-2023.

Author Contribution

Both authors contribute equally in all steps of the research and in reviewing the results, also, they have approved the final version of the manuscript before submission.

References

1. M. Kannadasan, Prem Kumar Bichala, Abhishek Agrawal. A Review: Nanoparticle drug delivery system. *IJPSM*.2020;5(12):46-58.
2. Areej W. Alhagies, Mowafaq M. Ghareeb. Formulation and characterization of nimodipine nanoparticles for the Enhancement of solubility and dissolution rate. *Iraqi J Pharm Sci*.2021;30(2):143-152.
3. Sabine Szunerits, Rabah Boukherroub. Heat: A Highly efficient skin enhancer for transdermal Drug Delivery. *Front. Bioeng. Biotechnol*. 2018; 6(15):1-13.
4. Hasanain Sh. Mahmood, Mowafaq M. Ghareeb, Zahraa Oleiwi Hamzah. Formulation and characterization of Flurbiprofen nanoparticles loaded microneedles. *Kerbala journal of pharmaceutical science*.2020;1(19):90-107.
5. Avcil M, Çelik A. Microneedles in drug delivery: progress and challenges. *Micro machines (Basel)*. 2021;12(11):1321.
6. Tejashree Waghule, Gautam Singhvi. Microneedles: A Smart approach and increasing Potential for Transdermal Drug Delivery System. *Biomed. Pharmacother.* 2019; 109:1249–1258.
7. Alimardani V, Abolmaali SS, Yousefi G. Microneedle arrays combined with nanomedicine approaches for Transdermal Delivery of Therapeutics. *J Clin Med*. 2021;10(2):181.
8. Sayani Bhattacharyya, Kavitha Hasabavi Kotresh. Microneedles- A new paradigm in transdermal delivery of therapeutic agents. *Pharm Sci Asia*. 2022; 49(5): 435-445.
9. Salwa, Chevala, Naga Thirumalesh. Polymeric microneedles for transdermal delivery of nanoparticles: frontiers of formulation, sterility and stability aspects. *J. Drug Deliv. Sci. Technol*. 2021; 65:102711.
10. Adeeb R. Alkhro, Mowafaq M. Ghareeb. Formulation and evaluation of iornoxicam as dissolving microneedle patch. *Iraqi J Pharm Sci*.2020;29(1):184-194.
11. Waghule T, Singhvi G, Dubey SK. Microneedles: A smart approach and increasing potential for transdermal drug delivery system. *Biomed Pharmacother*. 2019; 109:1249-58.
12. Zubiaur, Soria-Chacartegui, Villapalos-Garcia. The pharmacogenetics of treatment with olanzapine. *Pharmacogenomics*. 2021; 22(14):939 -958.
13. Somayeh Jafari, Francesca Fernandez-Enright, Xu-Feng Huang. Structural contributions of antipsychotic drugs to their therapeutic profiles and metabolic side effects. *J. Neurochem*. 2012; 120:371–384.
14. Rusul M. Alwan, Nawal A. Rajab. Nanosuspensions of selexipag: Formulation, characterization, and in vitro evaluation. *Iraqi J Pharm Sci*.2021;30(1):144-153.
15. Hamed HE, A. Hussein A. Preparation, in vitro and ex-vivo evaluation of mirtazapine nanosuspension and nanoparticles incorporated

- in orodispersible tablets. *Iraqi J Pharm Sci.* 2020;29(1):62–75.
16. Sreelola V, Sailaja AK, Pharmacy M. Preparation and characterisation of ibuprofen loaded polymeric nanoparticles by solvent evaporation technique. *Int J Pharm Pharm Sci.* 2014;6(8):416-21.
 17. Hasanain Sh. Mahmood, Mowafaq M. Ghareeb, Zahraa Oleiwi Hamzah. Formulation and in-vitro evaluation of flurbiprofen nanoparticles for transdermal delivery. *J Complement Med Res.* 2020;11(5):223.
 18. Rwaieda Adil Muhesen, Nawal Ayash Rajab. Formulation and characterization of olmesartan medoxomil as a nanoparticle. *Research J. Pharm. and Tech.* 2023 ;16(7):1-7.
 19. Sameer V. Dalvi, Rajesh N. Dave. Controlling particle size of a poorly water-soluble drug using ultrasound and stabilizers in antisolvent precipitation. *Ind. Eng. Chem. Res.* 2009;48(16):7581-7593.
 20. Nawal Ayash Rajab, Nizar Awish Jassem. A Design and in vitro evaluation of azilsartan medoxomil as a self-dispersible dry nanosuspension. *Der Pharmacia Sinica.* 2018; 9(1):12-322.
 21. Maher EM, Ali AM, Salem HF, Abdelrahman AA. In vitro/in vivo evaluation of an optimized fast dissolving oral film containing olanzapine co-amorphous dispersion with selected carboxylic acids. *Drug Deliv.* 2016;23(8):3088-3100.
 22. Adriano Antunes. Determination of the melting temperature, heat of fusion, and purity analysis of different samples of zidovudine using DSC. *Braz. J. Pharm. Sci.* 2010;46(1):38-43.
 23. Nikita Sehgal, Vishal Gupta N, Gowda DV. Fabrication and evaluation of solid dispersion containing Glibenclamide. *Asian J Pharm Clin Res.* 2018; 11(8): 158-61.
 24. Nawar M. Toma, Alaa A. Abdulrasool. Preparation and evaluation of microneedles-mediated transdermal delivery of montelukast sodium nanoparticles. *IJDDT.* 2021;11(3):1075-1082.
 25. Chu LY, Choi S-O, Prausnitz MR. Fabrication of dissolving polymer microneedles for controlled drug encapsulation and delivery: bubble and pedestal microneedle designs. *J. Pharm. Sci.* 2010;99(10):4228-4238.
 26. Amjed H. Noor, Mowafaq M. Ghareeb. Transdermal dissolvable microneedle-mediated delivery of controlled release ondansetron hydrogen chloride nanoparticles. *IJDDT.* 2021 ;11(3):859-863.
 27. He J, Zhang Z, Zheng X, Li L. Design and evaluation of dissolving microneedles for enhanced dermal delivery of propranolol hydrochloride. *Pharmaceutics.* 2021;13(4):579.
 28. Kamil K. Atiyah Altameemi, Shaimaa N. Abd-Alhammid. Anastrozole Nanoparticles for transdermal Delivery through microneedles: Preparation and evaluation. *J PHARM NEGATIVE RESULTS.* 2022; 13:974-980.
 29. Hayder Kadhim Drais, Ahmed Abbas Hussein. Investigation of lipid polymer hybrid nanocarriers for oral felodipine delivery: Formulation, method, in-vitro and ex-vivo evaluation. *Iraqi J Pharm Sci.* 2022;31(1):119-129.
 30. Rawaa M. Hussien, Mowafaq M. Ghareeb. Formulation and characterization of isradipine nanoparticle for dissolution enhancement. *Iraqi J Pharm Sci.* 2021;30(1):218-225.
 31. Danaei M, Dehghankhold M, Ataei S. Impact of particle size and polydispersity index on the clinical applications of lipidic nanocarrier systems. *Pharmaceutics.* 2018;10(2):57.
 32. Muneer R, Hashmet M.R, Pourafshary P. DLVO Modeling to predict critical salt concentration to initiate fines migration pre-and post-nano fluid treatment in sandstones. *SPE J.* 2022; 27:1915-1929.
 33. Leena Peltonen, Jouni Hirvonen. Pharmaceutical nanocrystals by nanomilling: critical process parameters, particle fracturing and stabilization methods. *J. Pharm. Pharmacol.* 2010. 62: 1569-1579.
 34. Li Xu, Zihan Chu, Jianhua Zhang. Steric effects in the deposition mode and drug-delivering efficiency of nanocapsule-based multilayer Films. *ACS Omega.* 2022;7(34): 30321-30332.
 35. Salatin S, Barar J, Barzegar-Jalali M. Development of a nanoprecipitation method for the entrapment of a very water soluble drug into Eudragit RL nanoparticles. *Res Pharm Sci.* 2017;12(1):1-14.
 36. Sara T. Ismail, Myasar M. Al-Kotaji, Ahlam A. Khayrallah. Formulation and evaluation of nystatin microparticles as a sustained release system. *Iraqi J Pharm Sci.* 2015;24(2):1-10.
 37. Cherukuri S, Batchu UR, Mandava K, Cherukuri V. Formulation and evaluation of transdermal drug delivery of topiramate. *Int J Pharm Investig.* 2017;7(1):10-17.
 38. Ahmed H. Ali, Shaimaa N. Abd-Alhammid. Enhancement of solubility and Improvement of dissolution rate of atorvastatin calcium prepared as nanosuspension. *Iraqi J PharmSci.* 2019;28(2):46-57.
 39. Yang H, Teng F, Wang P, Tian B. Investigation of a nanosuspension stabilized by Soluplus® to improve bioavailability. *Int J Pharm.* 2014; 30:477(1-2):88-95.
 40. Tiwari M, Chawla G, Bansal AK. Quantification of olanzapine polymorphs using powder X-ray diffraction technique. *J Pharm Biomed Anal.* 2007;43(3):865-72.

41. Cho H-W, Baek S-H, Lee B-J, Jin H-E. Orodispersible polymer films with the poorly water-soluble drug, olanzapine: hot-melt pneumatic extrusion for single-process 3D Printing. *Pharmaceutics*. 2020; 12(8):692.
42. Ajit Shankarrao K, Dhairysheel Mahadeo G. Formulation and in-vitro evaluation of orally disintegrating tablets of olanzapine-2-Hydroxypropyl- β -Cyclodextrin inclusion complex. *Iran J Pharm Res*. 2010;9(4):335.
43. Shashi Ravi Suman Rudrangi, Vivek Trivedi, John C Mitchell. Preparation of olanzapine and methyl--cyclodextrin complexes using a single-step, organic solvent-free supercritical fluid process: An approach to enhance the solubility and dissolution properties. *IJPR*. 2015;494(1):408-16.
44. Venkateskumar Krishnamoorthy, Suchandrasen, Verma Priya Ranjan Prasad. Physicochemical characterization and in vitro dissolution behavior of olanzapine-mannitol solid dispersions. *BJPS*. 2012;48(2): 244-255.
45. Yang S, Feng Y, Zhang L, Chen N. A scalable fabrication process of polymer microneedles. *Int J Nanomedicine*. 2012; 7:1415.
46. Lee JW, Park JH, Prausnitz MR. Dissolving microneedles for transdermal drug delivery. *Biomaterials*. 2008;29(13):2113-24.
47. Park JH, Allen MG, Prausnitz MR. Polymer microneedles for controlled-release drug delivery. *Pharmaceutical research*. 2006;23(5):1008-1019.
48. Baccaro S, Pajewski LA, Scoccia G. Mechanical properties of polyvinylpyrrolidone (PVP) hydrogels undergoing radiation. *Nucl Instrum Methods Phys Res B*. 1995;105(1-4):100-2.
49. Ahmed Saeed Al-Japairai K, Mahmood S, Hamed Almurisi S, Reddy Venugopal J. Current trends in polymer microneedle for transdermal drug delivery. *Int J Pharm*. 2020; 587:119673.
50. Tai A, Bianchini R, Jachowicz J. Texture analysis of cosmetic/pharmaceutical raw materials and formulations. *Int J Cosmet Sci*. 2014;36(4):291-304.
51. Shim WS, Hwang YM, Park SG. Role of polyvinylpyrrolidone in dissolving microneedle for efficient transdermal drug delivery: in vitro and clinical studies. *Bull Korean Chem Soc*. 2018;39 (6):789-93.

تصنيع وتقييم خلال الجلد الحي لإبرة مايكروية مذابة قائمة على جسيمات الأولانزابين النانوية للتوصيل عبر الجلد

أبو الفضل جابر نعمه الشيباني¹ و موفق محمد غريب^{2*}

¹ فرع الصيدلانيات، كلية الصيدلة، جامعة الكوفة، النجف، العراق
² فرع الصيدلانيات، كلية الصيدلة، جامعة بغداد، ابغداد، العراق

الخلاصة

أولانزابين (OLZ) يُصنف كدواء مضاد للذهان ويستخدم لعلاج الفصام، يمتلك توافر حيوي ضعيف ٦٠٪ بسبب قلة الذوبانية و الأبيض الكبدي للمرور الأول. لذلك، الهدف من العمل الحالي هو تصنيع وتقييم إبر دقيقة مذابة لجسيمات الأولانزابين النانوية للتوصيل عبر الجلد والتغلب على المشاكل المصاحبة لتناول الدواء عن طريق الفم، بالإضافة إلى سهولة إعطاء الدواء لمرضى الفصام. طريقة الترسيب النانوي استخدمت لتحضير جزيئات الأولانزابين النانوية باستخدام بوليمرات مختلفة و بنسب مختلفة. الجسيمات النانوية قُيِّمت من خلال العديد من دراسات التوصيف مثل حجم الجسيمات، مؤشر تعدد التشتت (PDI)، كفاءة الانحباس، جهد الزيتا ودراسة تحرر الدواء في المختبر. تم فحص شكل الجسيمات النانوية بواسطة المجهر الإلكتروني لمسح الانبعثات الميدانية (FESEM). تم تصنيع رقعة الإبرة المايكروية الذاتية (MN) عن طريق تحميل التشتت النانوي للأولانزابين في تجاويف القوالب الدقيقة من بولي ثنائي ميثيل سيلوكسان (PDMS)، متبوعة بصب المحلول البوليمري من البولي فينيل بيروليديون (PVP-K30) وكحول البولي فينيل (PVA) لتشكيل مصفوفة الإبرة المايكروية، رفع الإبرة الدقيقة المحضرة تم تقييمها من حيث الشكل والقوة الميكانيكية ومحتوى الدواء ودراسة النفاذية خلال جلد حي. أظهرت النتائج أن جسيمات الأولانزابين النانوية كانت بمقياس نانوي يتراوح من ٧٠،١٢ نانومتر إلى ٣٤٤ نانومتر، وتتراوح قيم PDI (٠،٤٠٤-٠،١٥٢) وتراوح كفاءة الانحباس من ٥٣،٢٪ إلى ٧٨،٤٪، وكانت أعلى قيمة جهد زيتا (-١٩،٠١ مللي فولت) لجسيمة الأولانزابين النانوية (OLZ-5)، التي أظهرت تحرر دواء هام وعالي ($P < 0.05$). يُظهر FESEM شكلاً كروياً للجسيمات النانوية بحجم مماثل لتلك التي تم الحصول عليها بواسطة زيتاسايزر. وفقاً لنتائج الجسيمات النانوية فإن الصيغة (OLZ-5) تعتبر صيغة محسنة وتستخدم في تصنيع الإبرة الدقيقة. نتائج تصنيع الإبرة المايكروية تشير إلى أن (MN-4) يُظهر إبر حادة ذات قوة ميكانيكية جيدة وفقاً لتحليل الملمس، ومحتوى دوائي عالٍ ٩٨،٥٢٪، دراسة النفاذية خلال الجلد الحي تشير إلى أن (MN-4) تنفذ خلال الجلد بشكل أكثر فعالية مقارنة بالرقعة البسيطة بنحو ٥،١٦ أضعاف. يمكن الاستنتاج بأن رقعة الإبرة الدقيقة (MN-4) تعتبر تركيبة واعدة للتغلب على المشاكل المرتبطة بتناول الدواء عن طريق الفم ويمكن أن يعزز توافره الحيوي، بالإضافة إلى تحسين امتثال المريض.

الكلمات المفتاحية: أولانزابين، جسيمات نانومترية، الذوبانية، بوليمرات، إبر دقيقة مذابة